An Efficient Workflow of Modeling Single-Nanowire Based Single-Photon Avalanche Detectors

Zhe Li*, H. Hoe Tan, Chennupati Jagadish, Lan Fu†
Department of Electronic Materials Engineering
Research School of Physics, The Australian National University, Canberra, Australia
email: *zhe.li@anu.edu.au; †lan.fu@anu.edu.au

***Abstract*—Single-photon detector (SPD) as an essential building block for detecting and counting photons, plays a fundamental role in quantum technologies. In this work, we propose an efficient workflow of modeling SPDs based on emerging one-dimensional materials, i.e. nanowires, utilizing avalanche breakdown in reverse biased condition. Comparing to another extensively studied platform, superconducting nanowire SPDs, avalanche nanowire device is demonstrated in this work to promise comparable performance (e.g. high photon detection efficiency (PDE) and and low dark count rate (DCR)) but without working at extreme cryogenic temperature (4K). The proposed workflow explored to maximize computational workload and balancing between time-consuming drift-diffusion simulation and fast script-based post-processing, and in timely convergence we were able to predict a suite of key performance metrics for single-photon SPDs, including breakdown voltage, PDE, DCR, and time resolution.**

***Index Terms*—single-photon detector, nanowire, TCAD, low-dimensional materials**

I. Introduction

Over the past two decades, various SPD device structures/technologies have been explored and developed [1], among which III-V compound semiconductor nanowires (NWs), due to their unique one-dimensional geometry, miniatured volume, and superior optical/electrical properties, have attracted intensive research for making next-generation high-performance single-photon avalanche photodetector (SPAD) [2]. Comparing to another extensively studied platform based on superconducting nanowire that requires cryogenic condition, avalanche NW device is demonstrated to promise competitive performance, but operating at much higher temperature [3]. However, to achieve high performance SPDs, it requires delicate control of growing well defined p-i-n junction with minimum bulk and surface defects; both doping and segment thickness of NWs play critical role in determining device performance. To provide timely guidance on material growth and device design, numerical modeling can help to optimise a range of structure parameters with negligible cost. However, a robust and efficient workflow to simulate a suite of key SPD performance metrics is still lacking, primarily because such modeling requires numerically stable solution beyond avalanche breakdown, which is challenging for the commonly used steady-state drift-diffusion (DD) scheme to converge due to high non-linearity in Geiger mode (e.g. [5]). Moreover, the electric field obtained from steady-state DD simulation is incorrect due to the lack of space-charge effects, which is why solution becomes easily diverging and simulated current tends to go to infinity. We thus propose a workflow based on solving time-dependent DD models, together with a range of auxiliary routines, such that breakdown voltage, time resolution, photon detection efficiency (PDE), and dark count rate (DCR), can be simulated in an integrated way with minimal computational workloads.

II. Numerical Methods and Workflow

The proposed simulation workflow combines both time-consuming time-dependent DD solver and fast script-based post-processing routines to predict four most important SPDs performance metrics, as detailed in Fig. 1. The DD solver in this work is implemented in COMSOL Multiphysics [4]. Time-dependent DD solver gives time-dependent current-voltage (IV) curves, from which avalanche built-up time can be extracted to calculate intrinsic time resolution of SPDs; it also generates spatial electric field to be used as input for fast post-processing routines. In parallel, a steady-state DD scheme is used to compute internal quantum efficiency (IQE), which is a much faster simulation since impact ionization model is disabled and just short-circuit condition (i.e. zero bias) is enough to compute IQE.

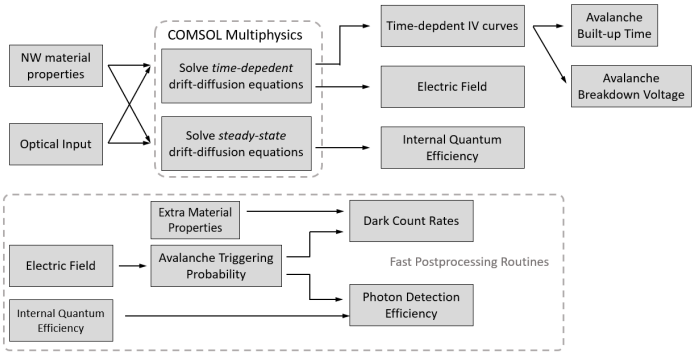

Fig. 1. Proposed hybrid workflow for modeling a suite of SPDs performance metrics.

Outside COMSOL workflow, exported electric field and IQE are used to compute other SPDs metrics. More specifically,

978-1-6654-7899-1/22/$31.00 ©2022 IEEE

following the scheme proposed in [6], the avalanche trigger probability (ATP) can be computed; combined with IQE, the photon detection efficiency (PDE) can be calculated. Given extra material properties (e.g. defect density) and carrier generate model (e.g. thermal or direct tunnelling), ATP can be used to calculate dark count rate (DCR).

III. Results and Discussions

To demonstrate the proposed workflow, we used SPD based on p-i-n homojunction InP NW as an example, assuming horizontally lying on a substrate with Ohmic contact at the tips of both p- and n-segments, which forms a 1D structure. The NW has a length of 3 μm, with a p-/n-, and i-doping of 10^{18} and 5×10^{15} cm^{-3}, respectively. The length of p-segment is fixed at 1 μm, while the length of i-region is varied from 250 to 1850 nm, with n-segment length changing correspondingly for fixed total NW length. The impact ionization model and parameters is based on [7], assuming operating temperature of 150K.

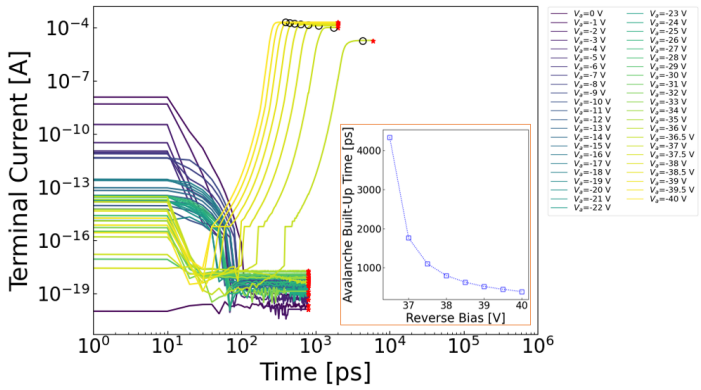

Fig. 2. Time-dependent IV curve for i-region thickness of 950 nm. Inset shows extracted avalanche built-up time against reverse bias.

Fig. 2 shows time-dependent IV curves for i-region thickness of 950 nm, where avalanche built-up time is highlighted in black circle and replotted in inset against bias beyond breakdown.

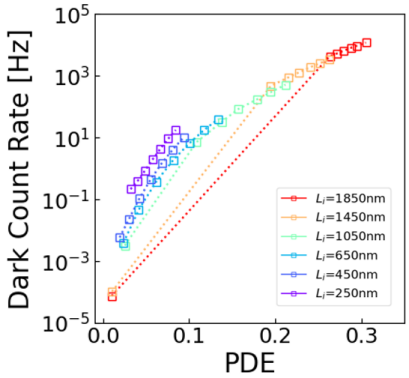

Fig. 3. Dark count rate (DCR) is plotted against length-averaged photon detection efficiency (PDE) for different i-region thickness.

Assuming high-quality InP NWs grown by selective-area epitaxy method [8] with a defect density of 10^{10} cm^{-3}, we can also compute DCR by including Shockley-Reed-Hall generation, trap-assisted and band-to-band tunneling generation [9]. Fig. 3 shows DCR against the length-averaged PDE, which is defined as $\langle \text{PDE} \rangle = L^{-1}\int_0^L \text{PDE}(x)dx$, where L is total NW length, and spatial PDE(x) is obtained assuming that a laser source of single-photon level excitation (5.6 pW) at 700 nm is scanned through NW. The trade-off that higher PDE induces larger DCR can be seen. Note that length-averaged $\langle \text{PDE} \rangle$ is only a conservative single-valued estimation while the peak PDE(x) can be much higher. The trade-off commonly seen in conventional bulk devices can be greatly suppressed in NW based device thanks to its miniatured volume. For example, for i-region thickness of 250 nm, it gives $\langle \text{PDE} \rangle$ around 10% (peak PDE ~40%) with DCR of ~10 Hz; in practice however, such performance may be compromised due to increased bulk and surface defects.

IV. Conclusion

We proposed a hybrid workflow to efficiently model single NW based SPDs. The approach utilizes time-dependent DD solver to model electric field beyond avalanche breakdown, obtaining time resolution and breakdown voltage. A much fast stationary DD solver is also set up to model IQE, and together with electric field, PDE and DCR can be readily computed using simple script-based routines with negligible computational cost. Lastly, an example demonstration also highlights the key advantage of exploring single NW based SPDs, where trade-offs between high PDE and large DCR can be effectively mitigated by optimizing i-region thickness.

Acknowledgment

The authors acknowledge the financial support from the Australian Research Council. This research was also undertaken with the assistance of resources and services from the National Computational Infrastructure (NCI), which is supported by the Australian government.

References

[1] C. J. Chunnilall, I. P. Degiovanni, S. Kück, I. Müller, A. G. Sinclair, Opt. Eng. 53(8) 081910 (10 July 2014)
[2] Wang, H., Guo, J., Miao, J., Luo, W., Gu, Y., Xie, R., Wang, F., Zhang, L., Wang, P., Hu, W., Small 2022, 18, 2103963.
[3] A. C. Farrell, X. Meng, D. Ren, et al., Nano Letters 2019 19 (1), 582-590.
[4] COMSOL Multiphysics, https://www.comsol.com
[5] Ansys Lumerical Support, https://support.lumerical.com/hc/en-us/articles/360042454814-Avalanche-photodetector. Accessed on May 17th, 2022.
[6] R. J. McIntyre, IEEE Transactions on Electron Devices, vol. 20, no. 7, pp. 637-641, July 1973.
[7] J. D. Petticrew, S. J. Dimler, C. H. Tan and J. S. Ng, Journal of Lightwave Technology, vol. 38, no. 4, pp. 961-965, 15 Feb.15, 2020.
[8] Gao, Q, Li, Z, Li, L, et al., Prog Photovolt Res Appl. 2019; 27: 237–244.
[9] J. P. Donnelly et al., IEEE Journal of Quantum Electronics, vol. 42, no. 8, pp. 797-809, Aug. 2006.